Experimental study of scattering from characterized random surfaces

K. A. O'Donnell* and E. R. Mendez†

Optics Section, Blackett Laboratory, Imperial College, London SW7 2BZ, United Kingdom

Received November 17, 1986; accepted February 11, 1987

An experimental investigation of light scattering from random rough surfaces is described. The surfaces, whose height fluctuations approximately follow Gaussian statistics, are fabricated in photoresist with a metal overcoating. When the lateral correlation length is larger than a wavelength and the surface slopes are mild, measurements of diffuse scattering are found to agree with the Beckmann theory, as long as the angle of incidence is not too large. For other surfaces that have stronger slopes, depolarization and enhanced backscattering may be observed in the diffuse scattering. Though we are unaware of theoretical calculations that compare with the measurements, the effects of multiple scattering are shown to be consistent with the major features of the observations.

1. INTRODUCTION

The scattering of electromagnetic waves from rough surfaces has been a subject of wide interest. A number of theoretical formulations of the rough-surface-scattering problem have appeared, some of which are quite formal in their approach. However, to make comparisons with experiments, any theory must determine the relationship between the characteristics of the random surface (that is, its height statistics and electromagnetic constants) and the statistical properties of the field scattered by it. As far as rigorous scattering theories are concerned, this problem has proved to be extremely difficult. A number of theoretical approaches with varying degrees of approximation have appeared, each of which has some range of applicability. Hence, in examining any surface-scattering theory, it is crucial to keep in mind what assumptions have been made and to ask how these assumptions may break down.[1] It is not yet clear when the various approximations hold or which theory would be better to explain the results of some experiments.

It has not been possible to obtain a general and analytical solution of the electromagnetic boundary conditions present on a rough surface, and to overcome this some approximations must be made. One formalism that has been used with some success is that of Beckmann and Spizzichino,[2] which uses the so-called Kirchhoff approximation. In this method, the total field and its normal derivative are approximated by the values that would exist on a plane tangent to each point of the surface. Though the Beckmann theory has the advantage that it leads to relatively straightforward calculations, it has well-known limitations. The Kirchhoff boundary conditions fail completely if the surface correlation scale a is comparable with the wavelength λ. Further, this theory does not take account of multiple scattering or surface shadowing, so for surfaces with steep slopes or at large angles the theory may also fail (though there have been attempts to include these effects in calculations[3,4]). Another method that is also used in rough-surface-scattering problems is the small-perturbation method of Rayleigh,[5] Fano,[6] and Rice.[7] In this approach, the solution is obtained by perturbing the planar solution in a power series of a roughness parameter. This method has its own limitations and is known to fail for deterministic surfaces with large slopes.[8] Its applicability to random surfaces should similarly be limited by the stochastic slopes, though it has never been made clear when results obtained with this technique are, in principle, valid.

More recently, another surface-scattering formulation that makes use of the Ewald–Oseen extinction theorem has appeared.[9–12] This approach has been applied to the case of perfectly conducting surfaces using both scalar[13,14] and vectorial[15] theories. For a perfect conductor, the extinction theorem mathematically represents the cancellation of the incident field inside the conductor by sources along the surface. This condition uniquely determines the electromagnetic boundary conditions so that, in principle, one may calculate the strength of the sources and then the scattered field outside the surface. The extinction-theorem method has the advantage that it puts no restrictions on the surface properties (such as the slopes or correlation scale) and that effects such as multiple scattering and shadowing are taken into consideration. However, in actual calculations, it is necessary to use a perturbation solution for the boundary conditions, of which only the first one or two terms may usually be calculated. Some of the solutions are thus limited to shallow surfaces with weak slopes, though the phase-perturbation technique[14] may have better (or certainly different) convergence properties for deeper surfaces.[16,17] Although the extinction theorem method is powerful, the practical numerical convergence of any results yet derived for a random surface, as far as we know, is an open issue.

There have been many experimental investigations of surface scattering, some of which we now describe, though we do not attempt to give an exhaustive discussion of that work here. Many different types of surface have been used, and the scattering properties that have been measured depend greatly on the concern of the investigators. Bennett and Porteus[18] and also Bennett[19] have found that the specular reflection of aluminized ground-glass surfaces follows approximately the exponential functional dependence on the roughness predicted by the theory of Davies.[20] Also, by employing ground-glass surfaces, Houchens and Herring[21] carried out a critical examination of theories based on the

0740-3232/87/071194-12$02.00

Kirchhoff approximation and concluded that the theory developed by Beckmann and Spizzichino[2] was more satisfactory than that of Davies. Further confirmations of the validity of the Beckmann theory were reported by Hensler,[22] who examined scattering from fused polycrystalline aluminum oxide surfaces. So, although it is not at all clear if the Kirchhoff boundary conditions are appropriate to deal with surfaces such as ground glass in the optical region, theories based on this approximation seem to predict reasonable results. Perhaps more challenging for the theoretical formulations are the experiments in which the surfaces contain subwavelength features or produce multiple scattering. Beaglehole and Hunderi[23] and Sari *et al.*[24] investigated the reflection and scattering properties of roughened metal foils with small transverse correlation lengths. Attempts have been made to fit the experimental data to the results of perturbation theories.[24–26] A great deal of experimental work applied to the characterization of optical surfaces is also reported in the literature.[27–31] For such surfaces, the roughness parameter is small, and the first-order Rayleigh vector perturbation theory seems to provide a method (at least one that gives self-consistent results) of finding the spectral density of the surface irregularities from measurements of the angular dependence of the scattered light. Also of interest is the work of Renau *et al.*,[32] who carried out an extensive study of scattering from several metallic and dielectric surfaces and in some cases found considerable amounts of depolarization and multiple scattering.

One general comment that we believe is significant is that, in many experiments, the surfaces are not well defined in a statistical sense. That is, fundamental quantities such as the height probability distribution and the transverse correlation function are not known or else are known imprecisely. Moreover, some surfaces have a wide range of length scales, and this may introduce complications into their characterization. For instance, in our experience, the features on the surface that cannot be resolved by the stylus tip of a profilometer modifies the output trace in an unpredictable way, so that one must then question the validity of the data. These considerations have led to difficulties in comparing experimental results with theoretical calculations, which, of course, must be evaluated for a given statistical surface model.

In what follows, we describe some experiments that attempt to alleviate this situation. The technique that we have used to fabricate surfaces should, within certain idealizations, lead to a surface that is a Gaussian *process*. In other words, the N-dimensional joint density of heights of the random surface is Gaussian for all N. It is significant that such Gaussian models are used extensively in theoretical calculations,[33] as they are a mathematically convenient model of a random surface. The quantity that we seek to measure in the present work is the mean diffusely scattered intensity, as this is often a central quantity of interest in both experiments and theoretical calculations. In a more general sense, the purpose of our experimental investigation is to see when existing surface-scattering theories may apply and to determine what occurs should they break down. For wavelengths λ that are available to us, we have fabricated surfaces whose correlation widths a are such that $a \gg \lambda$, so that some of the simpler theories may apply to them. Other surfaces have been fabricated such that $a \approx \lambda$ and $a < \lambda$, in which case more rigorous scattering formulations should be needed. However, it is not possible to predict whether existing scattering calculations will be applicable for the parameters of our surfaces.

The present work is organized as follows. In Section 2, the fabrication of the random surfaces is discussed, and the instrument used to measure the diffuse scatter is then described. Scattering data obtained with a diffuser having a wide correlation scale and shallow slopes are compared with the Beckmann theory in Section 3. Section 4 describes scattering from finer-scale diffusers that have stronger slopes. Measurements are discussed in detail and scattering models are developed in an effort to understand some of the observations. The results are summarized in Section 5, where conclusions are drawn on the relation of the measurements to existing theoretical scattering formulations.

2. THE RANDOM SURFACES AND THE SCATTERING INSTRUMENT

Fabricating the diffusers was one of the more difficult aspects of this work. The random surfaces were made in a manner that has been described by Gray.[34] Square glass plates of 50-mm width were spin-coated with high-resolution photoresist (Shipley 1375). Two or three layers were used to produce a net layer thickness of 10–14 μm. After drying and baking, the plates were exposed to laser speckle produced by a 0.457-μm argon-ion laser. A single speckle pattern ordinarily obeys negative exponential intensity statistics. Each plate was exposed, with equal exposure times, to a large number (N) of statistically independent speckle patterns, with the result that the net exposure approached that of a Gaussian process for large N (though for finite N it is more precisely a gamma-N process with point statistics following a gamma variate[35]). A typical total exposure time was 2 h. The plates were then processed in photoresist developer so as to produce a linear relation between exposure and surface height. As a final step, the developed plates were coated with a layer of gold or aluminum, using vacuum-coating methods. The metallic layer thickness is not known precisely but is estimated to be a few hundred nanometers; the surfaces were coated just sufficiently so that little light was transmitted through them. Electron micrographs comparing one of our diffusers with a ground-glass surface are shown in Fig. 1. The relatively smooth variations of the photoresist surface are seen to be quite different from the sharp edges present on the ground-glass surface.

For the diffusers to be described here, we used $N = 8$ independent speckle exposures. Fewer exposures caused departures from Gaussian statistics, while larger N leads to smaller height fluctuations for our fixed initial photoresist thickness. The lateral correlation function of the surface heights was determined by that of the exposing speckle pattern. We chose a Gaussian correlation not only because the rigorous theories are often evaluated for this case[33] but also because the laser used for exposure had a mode structure that leads to a Gaussian correlation of the exposing pattern. The standard deviation of surface heights (σ_h) was difficult to control precisely, though for a given diffuser care was taken that it was uniform over the surface. Surfaces that appeared to be satisfactory were scanned on a surface profi-

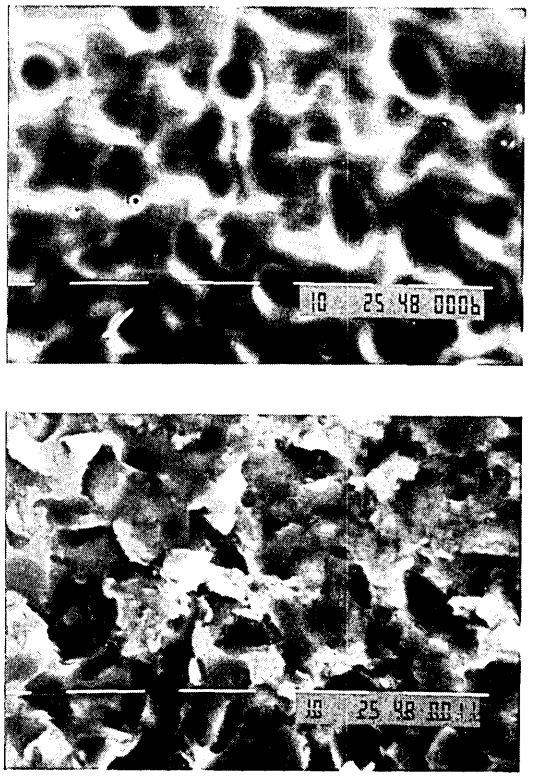

Fig. 1. Electron micrographs comparing one of the photoresist surfaces (diffuser #45, $a = 4.8$ μm, top) with a ground-glass surface (bottom). The length of the white lines is 10 μm.

lometer, using a mechanical stylus, and the data were analyzed statistically to see if they gave reasonable results.

Once the diffusers had been fabricated, an automated scattering instrument was used to measure their scattering properties. The three different sources that were used were a helium–neon laser ($\lambda = 0.633$ μm), an argon-ion laser ($\lambda = 0.514$ μm), and a carbon dioxide laser ($\lambda = 10.6$ μm). The optical geometry used was quite simple in concept and is shown in Fig. 2. To control the angle of incidence, the diffuser was mounted on a stage that allowed rotation about the vertical axis. The laser beam was sent through a periscope with two 45° mirrors, from which it left horizontally and was then incident upon the sample. The detector was mounted on a 62-cm-long arm that rotated about the sample in the horizontal plane. The measurements discussed here thus represent scattering in the plane of incidence. As shown in Fig. 2, the second mirror of the periscope occluded the detector when it was near the backscattering position, so this mirror was made as narrow as possible.

A typical measurement consisted of measuring the mean scattered intensity as a function of angle, for a fixed angle of incidence. Speckle is produced in the scattered field, and, to measure the mean intensity, it is necessary to average in some manner to reduce the speckle noise. This was achieved by illuminating an approximately 20-mm-diameter area of the scatterer (which creates small speckles), and by using a field lens at the detector that integrated over a fixed solid angle. Ideally, the field lens was much larger than a speckle yet smaller than structure present in the mean scattered field. Further, the field lens guaranteed that the detector viewed the entire illuminated area of the diffuser, irrespective of the angle of detection. A polarizer at the detector made it possible to measure the parallel- and orthogonal-polarization components should the sample cause depolarization. A small computer controlled the arm and sample stage so that data could be taken quickly and reproducibly.

There were some differences in the apparatus as set up for visible and infrared measurements. For reasons to become apparent later, measurements taken near backscattering in the visible were of interest, so it was desirable to make the second mirror of the periscope very narrow. This was achieved in this case by illuminating the sample with a slightly divergent beam, the focus of which was at the mirror. Simple calculations and measurements showed that this did not have a significant effect for the surfaces to be discussed here. In the infrared a slightly convergent beam was used that, when reflected from the sample, focused on the detector aperture. This was necessary because all the diffusers produced a strong specular component in the infrared, which is clearly separated from the diffuse component only at the focus of the beam. This geometry is also desirable in that the detector is strictly in the far field, but the blind spot in the backscattering direction was larger (4° as opposed to 1° in the visible). Because more spatial averaging was necessary in the infrared, a detector field lens of 20-mm diameter (about 2°) was used, while in the visible it was 10 mm (or 1°). In the visible system, direct detection with a photomultiplier (Hamamatsu R647) was possible. For the infrared work, a pyroelectric detector (Plessey PLT222) was used in conjunction with a chopper and a lock-in amplifier (Brookdeal 9503-SC).

It should be stressed that the data to be discussed represent the mean diffusely scattered signal, as a function of angle (relative to the mean diffuser surface), for a fixed solid angle of collection. No artificial angular factors are introduced into the data. As we have presented the data, a Lambertian diffuser would then produce a measured intensity that varied as the cosine of the scattering angle. We also do not attempt to place any absolute vertical scales on the data, although parallel and orthogonally polarized scattering components, on any given figure, are in their correct ratio.

To avoid confusion we also define the terminology used here to describe polarization. In reference to Fig. 2, we define s polarization as vertical and p polarization as horizontal (out of the plane of Fig. 2). This follows established

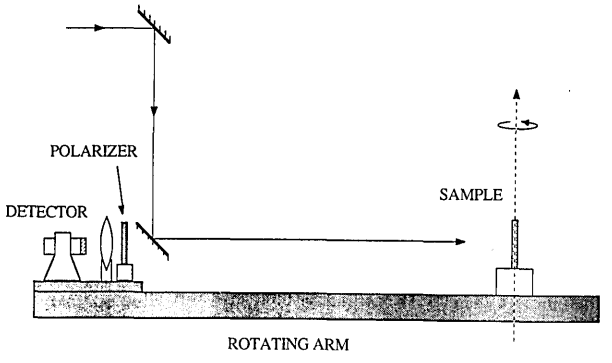

Fig. 2. A simplified diagram of the scattering instrument. The sample is rotated about the vertical axis to a fixed angle, and the detector arm then pivots about the same axis and records the angular dependence of the diffusely scattered intensity.

conventions for the case of diffuser tilts about the vertical axis (as will be the case here), though we use the above definitions even in normal incidence. This terminology is also used to define the direction of detected polarization. For example, *ss* data are taken with vertical incident and vertical detected polarization, and *sp* data are measured with similar incident but horizontal detected polarization.

3. SCATTERING RESULTS FOR A WIDE-SCALE SURFACE

In this section we present scattering measurements obtained using one of the widest-correlation-scale diffusers that has been made (diffuser #80, gold coated). For reasons to become clear later, this diffuser is the best characterized of the surfaces to be discussed here. A histogram of data taken with the surface profilometer is shown in Fig. 3. The fit of a Gaussian curve to the histogram is excellent, and the measured roughness standard deviation is $\sigma_h = 2.27$ μm. The correlation function of surface heights (Fig. 4) is also nearly Gaussian, with measured correlation width (hereafter defined as the e^{-1} half-width of the correlation) of $a = 20.9$ μm. This is in good agreement with the value $a = 21.9$ μm that had been estimated from the photoresist-exposing geometry.

What may be expected for the scattering properties of such a surface? First, for such a small ratio of σ_h/a, the slopes of the surface are quite modest. This implies that, from the standpoint of geometrical optics, multiple-scattering or shadowing effects will not be significant at small angles. Further, in the visible-wavelength range we have the condition $a \gg \lambda$, and at $\lambda = 10.6$ μm we find $a \approx 2\lambda$. As discussed in the introduction, the Beckmann theory should then clearly apply at visible wavelengths and may also apply at $\lambda = 10.6$ μm (though just what ratio of a/λ causes the theory to fail has never been made clear). In what follows, the data are compared with the Beckmann theory for the mean scattered intensity from a perfectly conducting Gaussian surface.[36] Because there has been controversy in the literature over the angular factors arising in the theory (Beckmann's F factor), we use the form derived by Nieto-Vesperinas,[37] which applies to the geometry of the experiment.

A measurement of the diffuse scattering at $\lambda = 0.633$ μm for an angle of incidence $\theta_i = 20°$ is shown in Fig. 5. It can be seen that the measurements are very smooth and have a Gaussian-like spread with symmetry about the direction of specular reflection. There was no observable depolarization, and the diffuser was too rough to produce a specular component. The solid curve is the Beckmann steepest-descent solution[38] for the diffuse component. It should be stressed that there was no arbitrary fitting of the theory to the data, as the two parameters required by the Beckmann theory (a and σ_h) were those values measured with the surface profilometer. The fit of the data to the theory is remarkably good. We believe that this is significant in that, to our knowledge, it represents the first experimental verification of the angular scattering predicted by the Beckmann theory with a well-defined surface. On the other hand, it may be shown that this theory effectively represents geometrical ray statistics for a surface rough compared with λ.[39] Thus, if one has faith in the theory, Fig. 5 could conversely

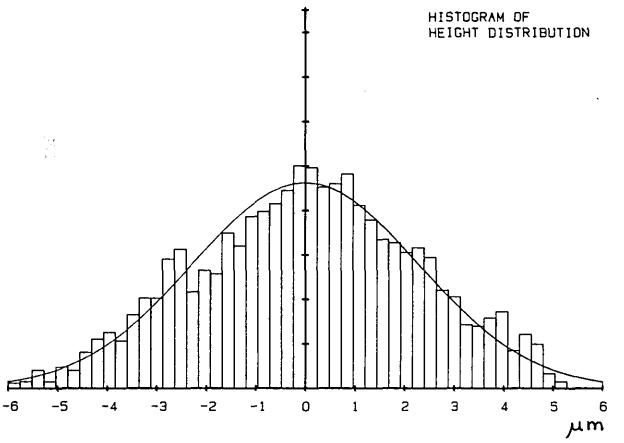

Fig. 3. Histogram of surface height data of diffuser #80 in comparison with a Gaussian distribution of the same variance. This was produced from 1000 measurements taken with a surface profilometer.

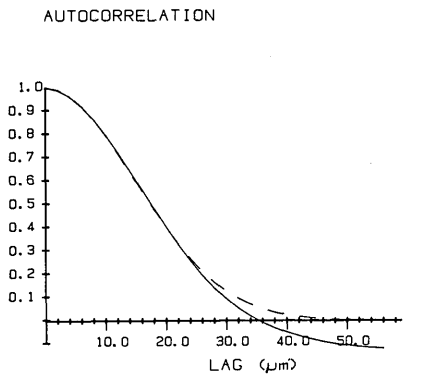

Fig. 4. Autocorrelation function (solid line) of profilometer surface height data of diffuser #80 as compared with a Gaussian function (dashed line).

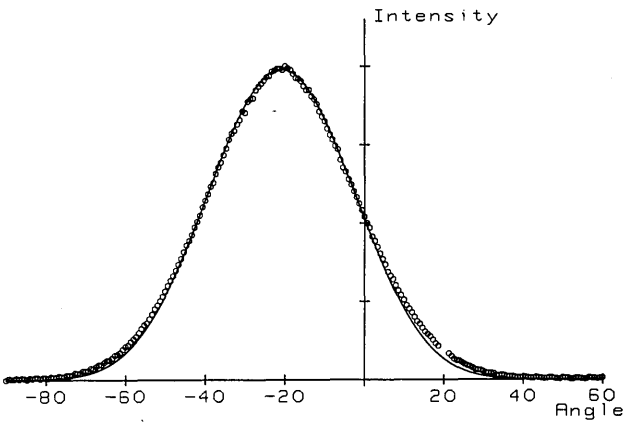

Fig. 5. Measured diffuse scattering from diffuser #80 with angle of incidence $\theta_i = 20°$, $\lambda = 0.633$ μm, and *s* incident polarization (no depolarization observed). The solid curve shows the Beckmann theory.

be taken as a verification that this surface has a slope distribution that is Gaussian, as should be the case for a Gaussian process.

Figure 6 shows a similar measurement of the diffuse scattering but with $\lambda = 10.6$ μm. Again no depolarization was observed, but there was a significant specular component (as the Beckmann theory predicts). The diffuse scattering is

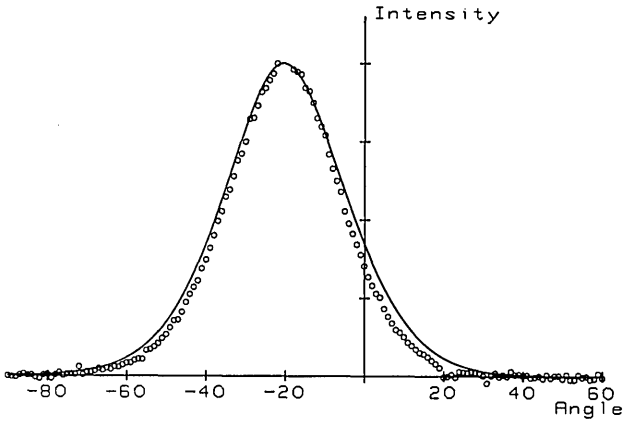

Fig. 6. Measured diffuse scattering from diffuser #80 with angle of incidence $\theta_i = 20°$, $\lambda = 10.6$ μm, and s incident polarization (no depolarization observed). The Beckmann theory is shown by the solid curve, and the specular component that was observed is not shown.

somewhat narrower than before but is still symmetric about scattering angle $\theta_s = -20°$. The solid curve is once again the Beckmann result, though for this wavelength the infinite series form of the solution is required.[40] The fit of data to theory is excellent, and, even with $a \approx 2\lambda$, the Beckmann solution works very well. However, a small but persistent tendency for the data to be narrower than the theory was seen in these and other data. This could conceivably be due to resonance effects (that is, $a \approx \lambda$), though further work would be needed to verify this.

We believe that it is remarkable how well the Beckmann theory works for these two measurements and in other scans for $\theta_i < 50°$, though further such data are not reproduced here. Under other experimental conditions it is a simple matter to observe results, even with this surface, that are in substantial disagreement with the Beckmann theory. The data shown in Fig. 7 are for diffuser #80 and $\lambda = 0.633$ μm but with incidence angle $\theta_i = 70°$. The measurements are now quite asymmetrical about the specular direction (denoted by the dashed line). The theory is still symmetrical about $\theta_s = -70°$, though it is unphysical in that it predicts scattering at $-90°$ and at angles behind the diffuser.

The Beckmann theory fails for this angle of incidence primarily because of shadowing and multiple scattering. One type of shadowing arises from the highest areas of the surface casting shadows at large incidence angles, though this is not important for $\theta_i = 70°$ and the parameters of this surface.[41] A second type of shadowing may also occur from the point of observation, in which some contributions to the light directed at the observation point are blocked by the surface and redirected elsewhere. This effect is most pronounced for scattering near $\theta_s = -90°$. This also implies that a significant amount of multiple scattering is occurring; the multiple scattering is also a consequence of the Beckmann theory's being nonzero at $\theta_s \leq -90°$. As noted earlier, the Beckmann theory is essentially geometrical at this wavelength so that scattering beyond $\theta_s = -90°$ represents rays that, after their first reflection from the random surface, are still traveling downward into the mean surface. These rays must strike the surface at least once more, and this simple theory does not attempt to take account of this.

As far as we know, there is no theory available to compare with our results. A theoretical explanation of these data must take into account the blocking of rays by the surface as well as their redirection. For the case of a Gaussian surface, Sancer[3] determined the effect on the ray statistics of removing the blocked rays, but, as Brown[42] has discussed, he did not include the effect of the redirection of rays. Because the Beckmann theory may still work at small angles, it has been fitted to the initial rise in the curve and works well to about $\theta_s = -50°$. As discussed above, the steep falloff of the data as θ_s approaches $-90°$ is due to shadowing, and the overshoot of the data near the specular direction is presumably due to the multiply scattered and hence redirected rays.

An unusual effect is shown in Fig. 8, which shows a measurement made with the same parameters as Fig. 7 but with $\lambda = 10.6$ μm. The specular component was quite strong at this angle, and the data points influenced by it have been omitted. It can be seen that the peak of the diffuse component lies inside the specular direction; this was observed numerous times for angles of incidence $\theta_i \geq 60°$. The Beckmann theory plotted shows a very similar peak shift. Though at $\lambda = 0.633$ μm the diffuse component has a geometrical interpretation and is then symmetrical, at $\lambda = 10.6$ μm the theory is diffractive. The series solution obtained by Beckmann in this case does not have symmetry about $\theta_s =$

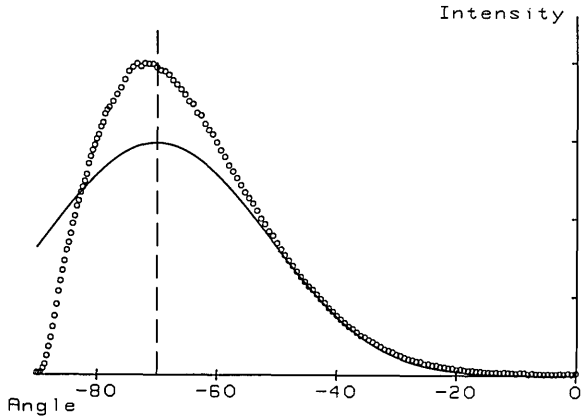

Fig. 7. Measured diffuse scattering from diffuser #80 with $\theta_i = 70°$, $\lambda = 0.633$ μm, and s incident polarization (no depolarization observed). The Beckmann theory (solid line) predicts scattering at $-90°$ and behind the diffuser.

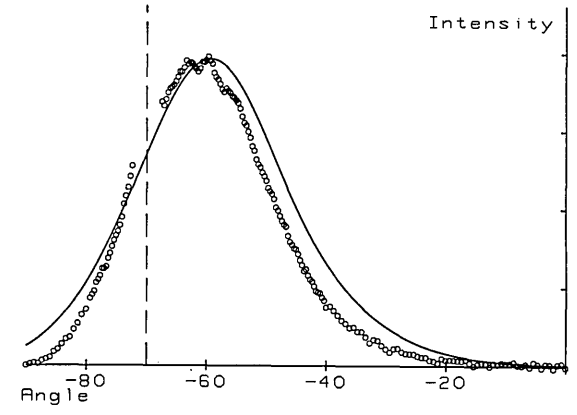

Fig. 8. Measured diffuse scattering from diffuser #80 with $\theta_i = 70°$, $\lambda = 10.6$ μm, and s incident polarization (no depolarization observed). The data and the Beckmann theory (solid line) are both skewed with respect to the direction of specular reflection (dashed line). The specular component is not shown.

$-\theta_i$, though earlier in Fig. 6 the skewness was not noticeable. It is perhaps surprising that for $a = 2\lambda$ and $\theta_i = 70°$ the agreement between theory and experiment is as good as it is, though it is difficult to determine whether the result is fortuitous.

4. SCATTERING RESULTS FROM FINE-SCALE SURFACES

In this section we describe results for considerably finer-scale diffusers. These surfaces, in both visible and infrared measurements, exhibited entirely different scattering behavior than did surfaces of the type described in the previous section. We have carried out a lengthy investigation of their scattering properties; only data that we consider most significant are presented here. Some preliminary work has been described in a previous paper.[43]

We first describe scattering measurements employing one of the smallest-scale diffusers that have yet been made (diffuser #83, gold coated, e^{-1} correlation width $a = 1.4$ μm). The fabrication of this surface was no more difficult than before, as photoresist has sufficient resolution to produce such small correlation scales. However, it was difficult to measure the height statistics of such a fine-scale surface directly. The stylus tip of the profilometer used has a width of ≈ 1 μm and does not accurately follow the surface contour, so the surface height data are not accurate. The slopes of the fine-scale surfaces are too strong for other profiling techniques (such as optical techniques), and it has not been possible to overcome this. The value that we quote for a is calculated from the measured parameters of the photoresist-exposing setup and appeared reasonable in comparison with electron-microscope observations. The value of σ_h is not well known for this surface, though we similarly estimate it as $\sigma_h \approx 1$ μm. In any case, diffuser #83 was sufficiently rough so that, in the visible, there was not any specular component in reflection (or in transmission before it was coated).

For this surface at visible wavelengths we have $a \approx 2\lambda$, which was the case in the previous section for diffuser #80 in the infrared. This does not imply, however, that results similar to those of the previous section should be expected, as the range of surface slopes present on these two diffusers is dramatically different. In the case of a Gaussian surface the slope s is a Gaussian variate with rms fluctuation $\sigma_s = \sqrt{2}\,\sigma_h/a$[44]; for diffuser #80, σ_s is then quite mild, though for #83 it could be of the order of unity. Not only do such steep slopes present problems for the available theoretical calculations but there could be considerable multiple-scattering and shadowing effects even near normal incidence.

Figure 9 shows the mean scattered intensity as a function of angle for $\lambda = 0.633$ μm, s incident polarization, and normal incidence. There are several remarkable aspects of these data. First, there is a great deal of depolarization, as the orthogonal sp component reaches about 50% of the ss component strength at some angles. Perhaps most unusual is the strong peak present at 0° in both the ss and the sp scattering, to either side of which are smaller secondary maxima. It should be stressed that the diffuser was considerably too rough for the central peak to be a specular reflection. The ss scattering has a slightly broader envelope than the sp component, and there are other small differences in the positions of

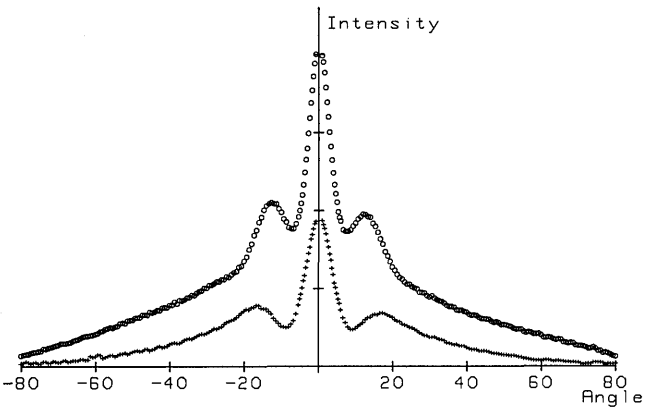

Fig. 9. Diffuse-scattering measurements from diffuser #83 with incidence angle $\theta_i = 0°$, $\lambda = 0.633$ μm, and s incident polarization. The O's denote the ss- (parallel-) and the +'s denote the sp- (orthogonal-) polarized scattering components.

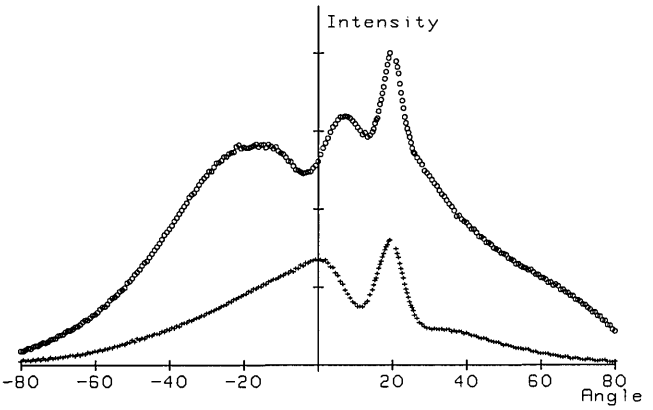

Fig. 10. Diffuse-scattering measurements from diffuser #83 with $\theta_i = 20°$, $\lambda = 0.633$ μm, and s incident polarization (the O's denote ss data and +'s denote sp data).

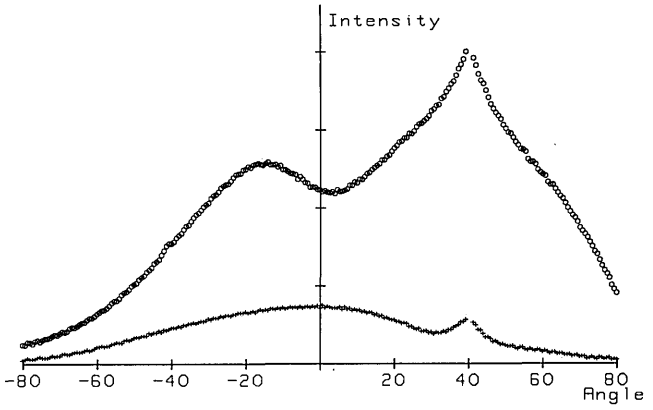

Fig. 11. Diffuse-scattering measurements from diffuser #83 with $\theta_i = 40°$, $\lambda = 0.633$ μm, and s incident polarization (the O's denote ss data and +'s denote sp data).

the secondary maxima. The scattering pattern is unusually narrow as compared with the surface slope distribution, so these results may not be explained as in Section 3.

Another peculiar property of diffuser #83 is illustrated in Figs. 10 and 11, which show scans of the scattered intensity for s polarization and incidence angles $\theta_i = 20°$ and 40°, respectively. There are no signs of a specular reflection, nor is there a symmetric diffuse component present at $\theta_s = -\theta_i$

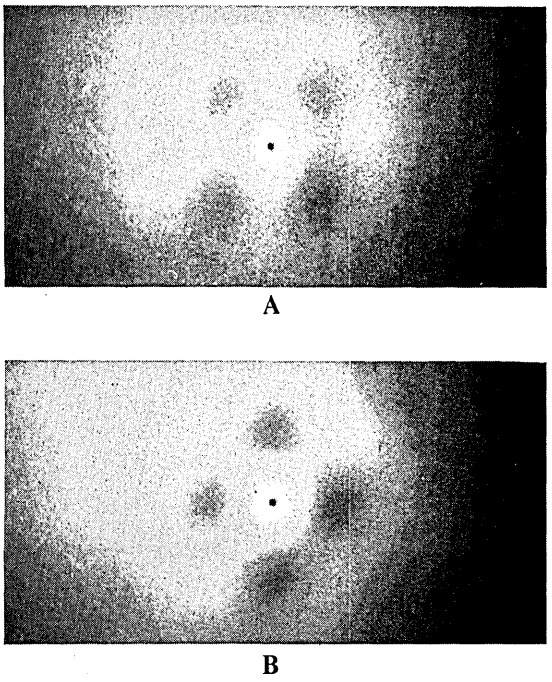

Fig. 12. Photographs of far-field scattering pattern in normal incidence from a fine-scale diffuser at $\lambda = 0.633$ μm. The incident polarization is vertical; A, parallel and B, orthogonally polarized scattering. The dark spot is a hole in the screen that lets the laser source through. Figures 9 and 17 correspond to scans of these patterns along the x and y axes, respectively.

(though there is a secondary peak there in Fig. 10). Instead, strong maxima fall at the exact backscattering direction in both the *ss* and the *sp* data. The secondary peaks of Fig. 9 first become skewed as the angle of incidence increases from 0°, until at 20° incidence the peak at one side has disappeared. At 40° incidence both secondary peaks have disappeared, and the backscattering peak has weakened slightly but is still quite distinct. Although the relative amount of depolarization also decreases as θ_i increases, there is still a significant amount of depolarization present in Figs. 9 and 10. Further measurements show that the enhanced backscattering is still observable at angles of incidence greater than 60°.

Other observations have shown that, even for normal incidence, the scattered intensity from diffuser #83 is not rotationally symmetric. This is not due to any lack of statistical isotropy in the surface (as may be checked by rotating the diffuser) but instead arises because of the polarization of the incident beam. Figure 12 shows photographs of the parallel and orthogonally polarized scattering for *s*-polarized incident light. The scattering patterns appear to have fourfold symmetry about the optical axis. The strongly enhanced backscattering is distinctly visible and is surrounded by an annular region containing highly polarization-dependent scattering.[45] There are four dark regions in this annulus, which rotate by 45° as the analyzer is rotated by 90°. Figure 9 corresponds to scans of Fig. 12 along the x axis, and this annular region falls at the angle where the minima appear in Fig. 9.

Similar behavior has been observed for all the fine-scale diffusers that have been fabricated ($a \approx 1.4$–1.8 μm). No surface-scattering theory known to us can account for the details of these observations, and it is unlikely that any of the rigorous theories cited earlier could be expected to apply. Nonetheless, we believe that it is possible to understand some of the physical mechanisms that give rise to the observations. In particular, the unusual aspects of the observations may be interpreted as arising because of a high degree of multiple scattering. Before this is discussed, we first digress to describe where similar phenomena involving enhanced backscatter have appeared previously. We then return to our observations and attempt to explain them, to some extent, using models of the scattering process. Later in the section, more data are presented, and the ways in which these compare with our models are discussed.

To our knowledge, enhanced backscattering has not been observed in rough-surface scatter before, although it has been noted in diverse circumstances in the past. Oetking[46] has found that many materials that are volume scatterers (such as MgO) may produce strong backscattering peaks for angles of incidence as large as 50°. His experiment was, in fact, an attempt to explain measurements dating back to the 1920's that showed an anomalously strong reflectance of the lunar surface near full moon. Egan and Hilgeman[47] have found similar backscattering effects in photometric standards and paints, and Becker *et al.*[48] have found unusually strong backscattering from soils at infrared wavelengths. It has been shown theoretically by de Wolf[49] that multiple scattering may lead to backscattering enhancement. This may provide an explanation of some of the above experimental observations. In studying scattering from dense suspensions of small particles, Kuga and Ishimaru[50] have presented strong experimental evidence that the enhanced backscattering that they observe arises solely because of multiple scattering, in accordance with the theory of Tsang and Ishimaru.[51] Further investigations of backscattering from particle suspensions have appeared,[52–55] largely because of its connection with analogous effects concerning multiple scattering of electrons from defects in solids.[56] It is interesting that enhanced backscattering was recently predicted theoretically in rough-surface scattering.[26,57] However, these calculations seem to apply only to surfaces with weak slopes and $\sigma_h \ll \lambda$, and the characteristics (and physical origins) of the backscattering enhancement appear to be different from our observations.

In a number of references, a simple and intuitive picture of the way in which multiple scattering may lead to backscattering enhancement has appeared.[56,58] To apply these ideas to a random rough surface, consider a multiple-scattering path that may occur in the valley of a surface, as shown in Fig. 13. In this figure, the incident field of wave vector $\mathbf{k}_i$ is initially scattered from point 1, then propagates to point 2,

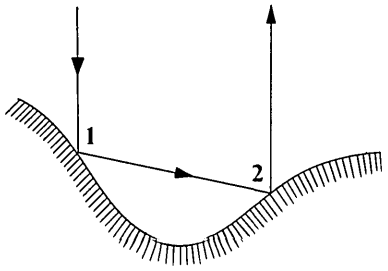

Fig. 13. A possible multiple-scattering path in a valley of the surface (see text).

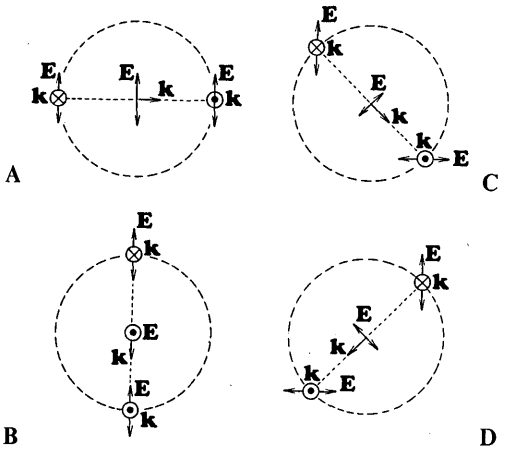

Fig. 14. Multiple scattering of polarized light from a valley in a two-dimensional surface, as seen from above in Fig. 13. For paths A and B there is no depolarization. In the case of a perfect conductor, paths C and D cross polarize the light that is returned. In the transverse paths of C and D the polarization vector is at 45° with respect to the plane of the figure.

and finally escapes from the surface with wave vector $\mathbf{k}_s$. Some of the incident field will follow the reversed path $2 \rightarrow 1$ and also contributes to the scattered field in the direction $\mathbf{k}_s$. If $\Delta\mathbf{r}$ is the vector from point 1 to point 2, the phase difference between these two paths is given by

$$\Delta\phi = (\mathbf{k}_i + \mathbf{k}_s) \cdot \Delta\mathbf{r}. \tag{1}$$

If $\mathbf{k}_s$ and $-\mathbf{k}_i$ are substantially different, averaging over all such multiple paths on a random surface (that is, with varying values of $\Delta\mathbf{r}$) will wash out any interference terms, and the forward and backward paths will contribute on an intensity basis to the mean intensity. However, when $\mathbf{k}_s \approx -\mathbf{k}_i$, the amplitude from such paired double-scattering paths will add constructively, and there will be a strong contribution to the mean intensity. The width of the backscattering peak may be found roughly by forming the average of Eq. (1) and requiring $\langle\Delta\phi\rangle$ to be less than 2π; this implies that the angular peak width $\Delta\theta_s$ is determined by

$$\Delta\theta_s \approx \lambda/w, \tag{2}$$

where w is the mean free path for the multiple scattering.

The polarization of the incident field should also be taken into account in the previous discussion. Consider the incidence of a vertically polarized plane wave upon a valley of a two-dimensional surface (Fig. 14). We consider, for simplicity, the surface to be composed of an array of planar mirrors. In this case, the polarization of a wave following a given path is determined by the (generally complex) reflectivities for s and p polarizations,[59] with respect to the local plane of incidence. The light following the double-scattering paths of Figs. 14A and 14B will not lead to any depolarization, as the light is purely s or p polarized. For the diagonal cross paths (Figs. 14C and 14D) the light has both s and p components; the complex reflectivities will lead, in general, to elliptical polarization in the returned light. In the case of a perfect conductor (as shown in Fig. 14), these diagonal paths cause a rotation of the polarization vector by 90°, and the light is returned cross polarized.

Direct observations of light reflected from the surface have been made that are entirely consistent with the above discussions. In Fig. 15, photographs of one of the surfaces (diffuser #45) taken in an optical microscope (N.A. = 0.80, 50×) with vertical incident polarization are shown. The two photos are of the same area, but one is taken through a parallel analyzer and the other with a crossed analyzer. The regions where the strongest depolarization is observed (see the circled areas) are believed to be valleys in the surface. In each such region, there is an annular pattern having four dark spots at the positions where the light should be most strongly polarized, as in Figs. 14A and 14B. When the analyzer is rotated by 90° and the polarized scattering is viewed, the four spots rotate by only 45° and appear at the positions of Figs. 14C and 14D (though these spots are difficult to see in the photo). Moreover, the contrast of the patterns is less in this case, presumably because the gold surface leads to some degree of elliptical polarization of the diagonal cross paths. It is also possible to demonstrate explicitly that these patterns are due to multiple scattering. This may be done by scanning a step function of intensity across the viewing field of the microscope. If the scanning is done, for the sake of argument, from right to left, the patterns from the valleys become dark from left to right, which is consistent with the light paths of Fig. 14.

These observations are helpful in interpreting various aspects of the far-field scattering pattern. As can be seen from Fig. 14, the multiple scattering in a valley has a fourfold symmetry for a perfect conductor. Propagation of the two polarization components to the far field will then lead to the apparent fourfold symmetry of Fig. 12 (though the effects of real metals will be discussed later). Further, the stronger contrast of the depolarized surface patterns in Fig. 15 leads to the higher contrast of this component in Fig. 12. The dark patches in Fig. 12 are presumably the first diffraction minimum of the multiple-scattering paths. The first minimum of the *ss* scan in Fig. 9 falls at about 8°; this implies an approximate mean free path of $w \approx 4.5$ μm from Eq. (2),

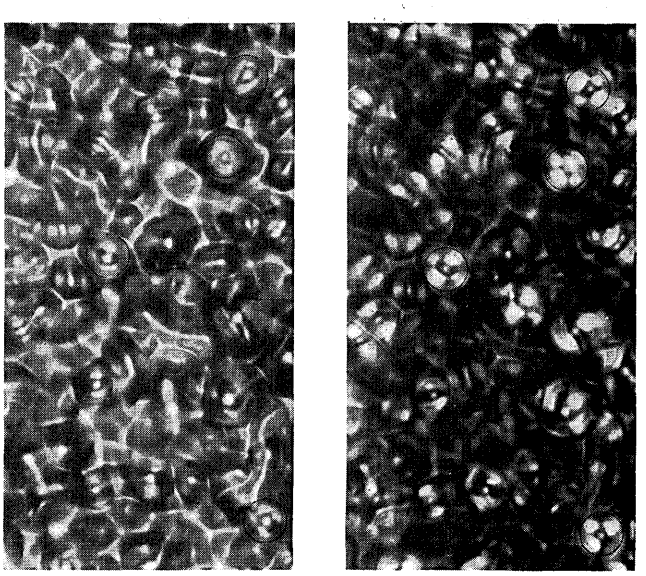

Fig. 15. Optical micrographs (N.A. = 0.80, 50×) of the same area of diffuser #45 with linearly polarized illumination and viewed with a parallel (left) and perpendicular (right) analyzer. The areas where depolarization is observed (see circles) exhibit patterns analogous to Fig. 14.

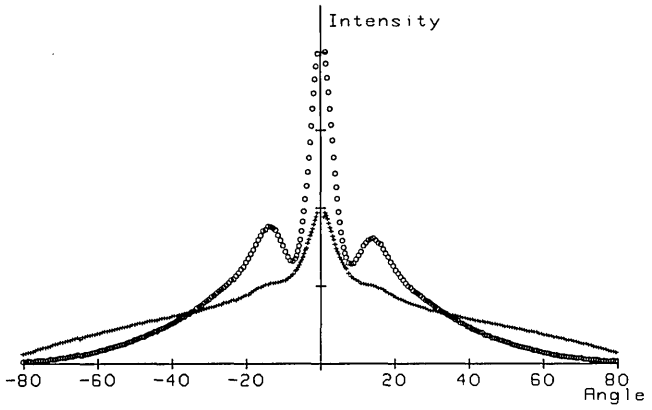

Fig. 16. Diffuse scattering from diffuser #83, incidence angle θ_i = 0°, λ = 0.633 μm, and RHCP incident polarization. The O's denote RHCP and the +'s denote LHCP-detected radiation.

which is roughly the size of the multiple-scattering regions of Fig. 15.

It also should be stressed at this point that the above discussions involve idealized models, which cannot be expected to explain all the observations. Even within the constraints of the locally planar surface model (itself perhaps a dubious assumption), the surface patterns as shown in Fig. 15 are by no means circular and take on a range of distorted shapes for a random surface. Hence these models are presented here only in an attempt to interpret the major features of the scattering, and no claim is made regarding whether such models may provide quantitative agreement with the observations.

We now return to discuss further experimental measurements. It is possible, to some degree, to isolate the double scattering from the single scattering, as has been discussed by Etemad *et al.*[55] If the diffuser is illuminated with right-handed circularly polarized (RHCP) radiation, the odd-order scattering is largely returned with left-handed circular polarization (LHCP), while the even-order scattering is mostly returned as RHCP radiation. A measurement made with diffuser #83 in normal incidence with RHCP light is shown in Fig. 16. It can be seen that the RHCP component has an unusually high central peak and strong secondary maxima, which suggests that double scattering produces most of the backscatter. The LHCP component has a wide envelope, which may be associated with single scattering. There is, perhaps surprisingly, a small backscattering peak in the LHCP component without sidelobes. This could arise from depolarization in the double scattering owing to the finite conductivity of the surface, though another interesting possibility is that it may be due to a small amount of triple scattering. In any case, the great disparity in the backscattered heights for the two components suggests that the backscattering is due largely to double scattering.

It is also possible to demonstrate that the far-field intensity does not quite have fourfold symmetry. In Fig. 17 is shown the mean scattered intensity of diffuser #83 in normal incidence but with *p* incident polarization. This corresponds to scans of the patterns of Fig. 12 along the *y* axis. In comparing these measurements with Fig. 9, it may be seen that the *ps* and *sp* components are nearly identical. However, the other components differ in that Fig. 9 has distinct secondary maxima in the *ss* component, while Fig. 17 shows weaker scattering at these angles without such maxima in the *pp* data. Similar effects have been found for other fine-scale diffusers that have been made, though secondary maxima are sometimes found in the *pp* scans, but they are always weaker than those in the *ss* data. Although the fourfold symmetry occurs in the scattering paths of Fig. 14 for a perfect conductor, this is not to be expected for a real metal. This may be seen easily in the paths of Figs. 14A and 14B, for one involves the *s* and the other the *p* reflectivity; these are different for real metals and violates the earlier symmetry. Hence these measurements are not necessarily surprising, though whether the above discussion is adequate or the explanation is more subtle will not be pursued here. In passing, we also note that small differences have been obtained with *p*-polarized illumination at nonnormal incidence, as compared with Figs. 10 and 11, though this is not presented here.

Surfaces have also been fabricated that exhibit enhanced backscattering to a lesser degree than diffuser #83. Diffuser #45 is an example of such a surface. The profilometer gave values of σ_h = 0.93 μm and a = 4.6 μm for this diffuser (compared with a = 4.8 μm from the exposing parameters); this value of a is large enough compared with the stylus width so that the surface profilometer results may be reasonably trustworthy. The mean intensity scattered from this diffuser for *s* incident polarization is shown in Figs. 18 and 19 for angles of incidence 0° and 20°, respectively. It may be seen that there are still significant backscattering effects and depolarization, though these effects are weaker than for diffuser #83. Further, the angular width of the backscattering structure is narrower, which should be expected for a surface with a larger correlation scale and hence mean free path for multiple scattering. The extremely broad scattering pattern in Fig. 18 is probably associated with single scattering, which measurements using RHCP illumination have suggested, though we do not reproduce this here. Further evidence of this is shown in Fig. 19. As is often found for single-scattering theories, the peak of the polarized scattering falls near the angle of specular reflection. Hence this diffuser is an example of a surface that, in its scattering characteristics, is intermediate between diffusers #80 and #83. It is interesting that diffuser #45 has considerably weaker slopes than diffuser #83 but gives rise to a much wider scattering pattern. This is possibly because the angu-

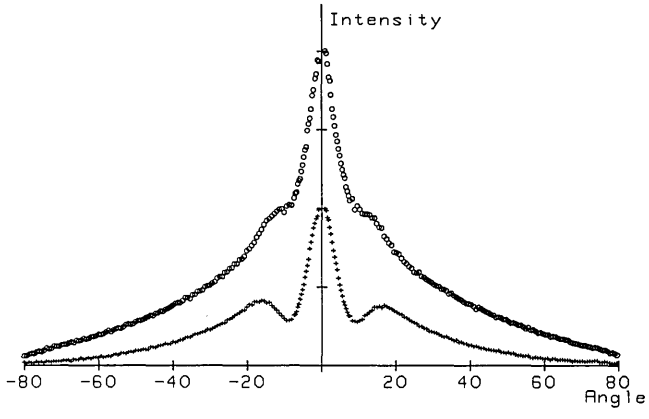

Fig. 17. Diffuse-scattering measurements from diffuser #83 with incidence angle θ_i = 0°, λ = 0.633 μm, and *p* incident polarization (the O's denote *pp* and +'s denote *ps* scattering).

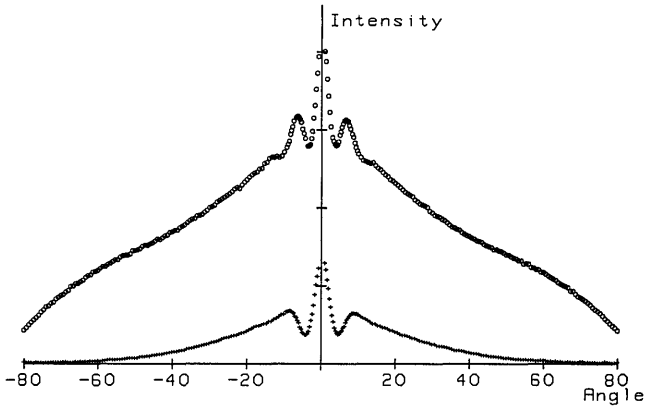

Fig. 18. Diffuse-scattering measurements from diffuser #45 with $\theta_i = 0°$, $\lambda = 0.633$ μm, and *s* incident polarization. The O's denote *ss* scattering and +'s denote *sp* scattering.

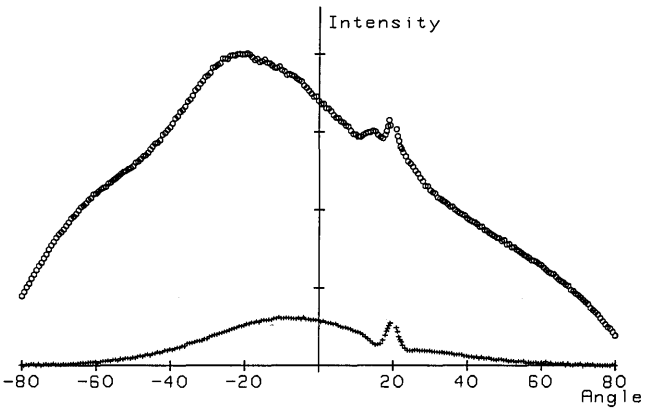

Fig. 19. Diffuse-scattering measurements from diffuser #45 with $\theta_i = 20°$, $\lambda = 0.633$ μm, and *s* incident polarization. The O's denote *ss* and the +'s denote *sp* data.

lar scatter more closely reflects the slope distribution of diffuser #45; so much backscattering occurred for #83 that its pattern was very narrow.

A comparison of measurements made at red ($\lambda = 0.633$ μm) and green ($\lambda = 0.514$ μm) wavelengths with diffuser #45 in normal incidence is shown in Fig. 20. These data are normalized to show the relative strengths of features at different wavelengths. The vertical scale at a given wavelength has been determined as follows. The total intensity for a given λ (polarized plus depolarized values) was assumed to be rotationally symmetric; this was then integrated over the entire solid angle to find the net scattered power. The scans at that wavelength were then divided by the power that was calculated; the resulting data are then normalized as in a probability density. The assumption of circular symmetry is, of course, not strictly valid; but we believe the errors resulting from this are smaller than the differences apparent in Fig. 20.

First, in Fig. 20 the width of the backscattering structure is narrower for the green measurement than in the red case, but this is not surprising because of the wavelength scaling of features predicted by expression (2). What is more interesting is the relative strength of the backscattering effects. This is most clearly seen in the *sp* components, for which the red scattering, at some angles, is more than twice as strong as the green curve. A possible interpretation of this may be understood in reference to Fig. 13. As $\lambda \to 0$, the multiple-scattering paths between points 1 and 2 will obey geometrical optics. Hence any backscattered intensity will arise solely from pairs of surface facets that send rays back toward the source. If wave effects are significant, surface elements diffract light to a spread of angles about the geometrical direction, and, as λ increases, these diffraction widths increase. Thus, as the geometrical-optics conditions are relaxed, larger areas on opposing sides of the valley in Fig. 13

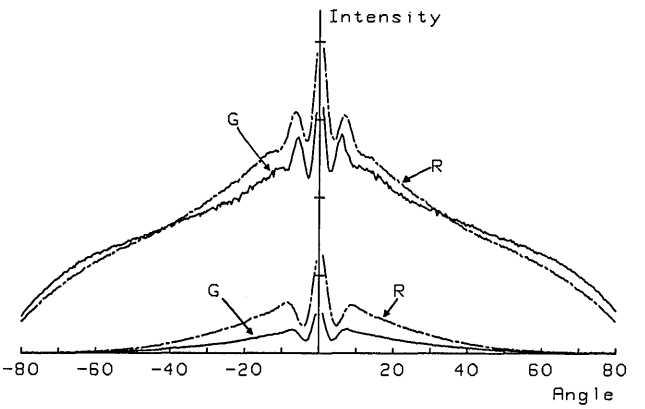

Fig. 20. Measured diffuse scattering from diffuser #45 in normal incidence, $\lambda = 0.514$ μm (G), and $\lambda = 0.633$ μm (R), normalized to show relative strengths as discussed in the text. The upper two curves are the *ss* components, and the lower pair are the *sp* data.

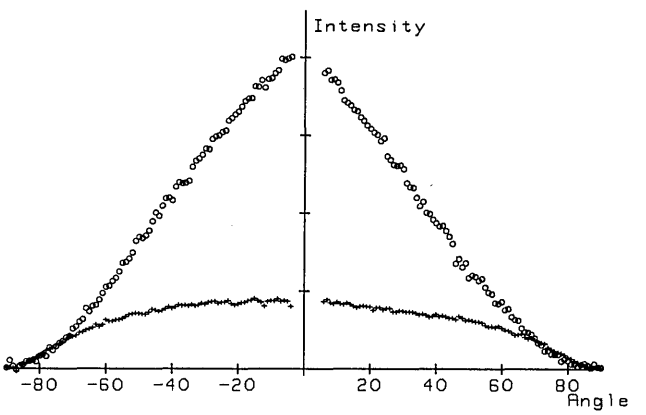

Fig. 21. Diffuse-scattering measurements from diffuser #83 with $\theta_i = 0°$, $\lambda = 10.6$ μm, and *s* incident polarization (O's denote *ss* data and +'s denote *sp* data).

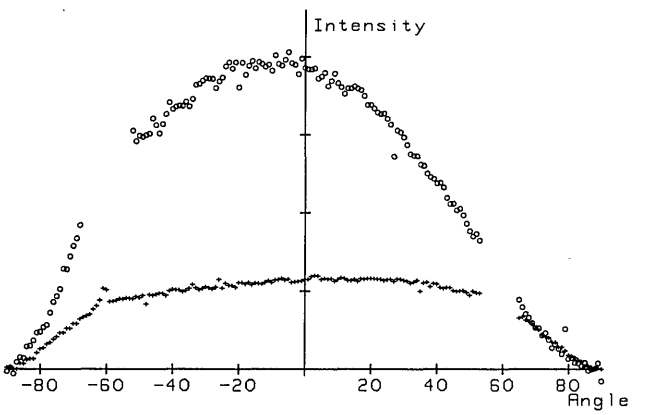

Fig. 22. Diffuse scattering from diffuser #83 with $\theta_i = 60°$, $\lambda = 10.6$ μm, and *s* incident polarization (the O's denote *ss* and +'s denote *sp* data).

will contribute to multiple scattering, so the increase of the backscattering strength is not unreasonable for longer wavelengths. It is remarkable, however, that such a small-wavelength shift produces an increase in the enhanced backscattered intensity by a factor of approximately 2.

This model will eventually break down, because as λ becomes larger the structure of the valleys will not be seen by the wave, and the simple model of Fig. 13 will break down completely. Such is the case with diffusers #45 and #83 and 10.6-μm radiation. In this case we have not observed any enhanced backscattering, even in scans through $\theta_s = 0°$ using a beam splitter. Scans made with diffuser #83 at normal and 60° incidence are shown in Figs. 21 and 22. In both cases there was a strong specular component that is not shown in these figures. It can be seen that for $\theta_i = 0°$ the curves are very broad, have about 20% depolarization, and show no unusual structure in the scattered field. Figure 22 is interesting in that there is little skewness in the diffuse scattering for an incidence angle as large as 60°, and the relative amount of depolarization has actually increased slightly. Similar results have been obtained in the infrared for diffuser #45, though the depolarization is weaker. We do not know of any theory that claims to be valid for surfaces with steep slopes and $a \ll \lambda$, and, although these results are unusual and deserve more attention, we do not attempt to present an interpretation of them.

5. DISCUSSION AND CONCLUSIONS

In this work we have studied the diffuse-scattering properties of characterized random surfaces, and a wide range of scattering behavior has been observed. When the correlation scale a of the surface was greater than λ and the surface slopes were modest, good agreement with the Beckmann theory has been obtained for small angles of incidence. This in itself is significant because this theory has not, to our knowledge, been tested with a surface of known statistics. Even though the experiment disagrees with the theory at large angles of incidence, this behavior is, to some extent, understood. However, the scattering characteristics measured in other cases have been unusual. For surfaces with $a \approx 2\lambda$ and strong surface slopes, depolarization and strongly enhanced backscattering have been observed. We have attributed this behavior to multiple scattering, but the scattering characteristics that we observe have not been predicted by any theory known to us. It is quite reasonable to ask why these effects have been observed here and have not been noted before in surface scattering. We believe that the reason lies in the nature of our surfaces. These surfaces, with relatively deep valleys a few wavelengths across, seem to lead to quite strong multiple-scattering effects. Much other surface-scattering work has been based on randomly ground surfaces; these surfaces are inevitably somewhat poorly characterized, but they do not seem to lead to the same degree of multiple scattering.

The discussion of the depolarization and backscattering enhancement that we have presented has been largely qualitative, as models have been developed that seem to account for the major features of the observations. Such models, however, cannot produce quantitative results, and we believe that many questions concerning our observations remain unanswered. In particular, the quantitative dependence of the observed effects on the surface parameters and illumination wavelength awaits the development of rigorous calculations. Despite much effort in surface-scattering theory in recent years, further research is needed to compare theory with experiment. Indeed, before a thorough understanding of surface scattering is reached, it may be said that considerable progress must still be made in both theoretical and experimental areas. It is hoped that the present work will stimulate further such research.

ACKNOWLEDGMENTS

Throughout the course of this research, we have been grateful for discussions with and the help of J. C. Dainty, F. C. Reavell, A. S. Harley, M. J. Kim, and A. Canas on various aspects of this work. The financial support for this project was provided by the U.K. Science and Engineering Research Council under grants GRD/91048 and GRD/60997.

* Current address, Dipartimento di Fisica, Università degli Studi, Fisica Superiore, Via S. Marta No. 3, Florence, Italy.

† Current address, Departamento de Fisica, Universidad Autonoma Metropolitana, 09340 Mexico D.F., Mexico.

REFERENCES AND NOTES

1. G. S. Brown, "A comparison of approximate theories for scattering from random rough surfaces," Wave Motion **7**, 195–205 (1985).
2. P. Beckmann and A. Spizzichino, *The Scattering of Electromagnetic Waves from Rough Surfaces* (Pergamon, New York, 1963).
3. M. I. Sancer, "Shadow-corrected electromagnetic scattering from a randomly rough surface," IEEE Trans. Antennas Propag. **AP-17**, 577–585 (1969).
4. A. K. Fung and H. J. Eom, "Multiple scattering and depolarization by a randomly rough Kirchhoff surface," IEEE Trans. Antennas Propag. **AP-29**, 463–471 (1981).
5. Lord Rayleigh, *The Theory of Sound* (Dover, New York, 1945), Vol. 2.
6. U. Fano, "The theory of anomalous diffraction gratings and of quasi-stationary waves on metallic surfaces (Sommerfeld's waves)," J. Opt. Soc. Am. **31**, 213–222 (1941).
7. S. O. Rice, "Reflection of electromagnetic waves from slightly rough surfaces," Commun. Pure Appl. Math. **4**, 351–378 (1951).
8. R. F. Millar, "The Rayleigh hypothesis and a related least-squares solution to scattering problems for periodic surfaces and other scatterers," Radio Sci. **8**, 785–796 (1973).
9. D. N. Pattanayak and E. Wolf, "General form and a new interpretation of the Ewald–Oseen extinction theorem," Opt. Commun. **6**, 217–220 (1972).
10. G. S. Agarwal, "Scattering from rough surfaces," Opt. Commun. **14**, 161–166 (1975).
11. G. S. Agarwal, "Interaction of electromagnetic waves at rough dielectric surfaces," Phys. Rev. B **15**, 2371–2383 (1977).
12. P. C. Waterman, "Scattering from periodic surfaces," J. Acoust. Soc. Am. **57**, 791–802 (1975).
13. M. Nieto-Vesperinas and N. Garcia, "A detailed study of the scattering of scalar waves from random rough surfaces," Opt. Acta **28**, 1651–1672 (1981).
14. J. Shen and A. A. Maradudin, "Multiple scattering of waves from random rough surfaces," Phys. Rev. B **22**, 4234–4240 (1980).
15. M. Nieto-Vesperinas, "Depolarization of electromagnetic waves scattered from slightly rough random surfaces: a study by means of the extinction theorem," J. Opt. Soc. Am. **72**, 539–547 (1982).

16. D. Winebrenner and A. Ishimaru, "Investigation of the surface field phase-perturbation technique for scattering from rough surfaces," Radio Sci. **20,** 161–170 (1985).
17. D. Winebrenner and A. Ishimaru, "Application of the phase-perturbation technique to randomly rough surfaces," J. Opt. Soc. Am. A **2,** 2285–2294 (1985).
18. H. E. Bennett and J. O. Porteus, "Relation between surface roughness and specular reflectance at normal incidence," J. Opt. Soc. Am. **51,** 123–129 (1963).
19. H. E. Bennett, "Specular reflectance of aluminized ground glass and the height distribution of surface irregularities," J. Opt. Soc. Am. **53,** 1389–1394 (1963).
20. H. Davies, "The reflection of electromagnetic waves from a rough surface," Proc. Inst. Electr. Eng. **101,** 209–214 (1954).
21. A. F. Houchens and R. G. Herring, "Bidirectional reflectance of rough metal surfaces," Prog. Astronaut. Aeronaut. **20,** 65–89 (1967).
22. D. H. Hensler, "Light scattering from fused polycrystalline aluminum oxide surfaces," Appl. Opt. **11,** 2522–2528 (1972).
23. D. Beaglehole and O. Hunderi, "Study of the interaction of light with rough metal surfaces. I. Experiment," Phys. Rev. B **2,** 309–321 (1970).
24. S. O. Sari, D. K. Cohen, and K. D. Scherkoske, "Study of surface plasma-wave reflectance and roughness-induced scattering in silver foils," Phys. Rev. B **21,** 2162–2174 (1980).
25. O. Hunderi and D. Beaglehole, "Study of the interaction of light with rough metal surfaces. II. Theory," Phys. Rev. B **2,** 321–329 (1970).
26. V. Celli, A. A. Maradudin, A. M. Marvin, and A. R. McGurn, "Some aspects of light scattering from a randomly rough metal surface," J. Opt. Soc. Am. A **2,** 2225–2239 (1985).
27. J. M. Elson, H. E. Bennett, and J. M. Bennett, "Scattering from optical surfaces," in *Applied Optics and Optical Engineering,* R. R. Shannon and J. C. Wyant, eds. (Academic, New York, 1979), Vol. VII.
28. E. L. Church, H. A. Jenkinson, and J. M. Zavada, "Measurement of the finish of diamond-turned metal surfaces by differential light scattering," Opt. Eng. **16,** 360–374 (1977).
29. E. L. Church, H. A. Jenkinson, and J. M. Zavada, "Relationship between surface scattering and microtopographic features," Opt. Eng. **18,** 125–136 (1979).
30. J. C. Stover, S. A. Serati, and C. H. Gillespie, "Calculation of surface statistics from light scatter," Opt. Eng. **23,** 406–412 (1984).
31. P. Roche and E. Pelletier, "Characterization of optical surfaces by measurement of scattering distribution," Appl. Opt. **23,** 3561–3566 (1984).
32. J. Renau, P. K. Cheo, and H. G. Cooper, "Depolarization of linearly polarized electromagnetic waves backscattered from rough metals and inhomogeneous dielectrics," J. Opt. Soc. Am. **57,** 459–467 (1967).
33. See Refs. 2, 13, 14, 15, and 26.
34. P. F. Gray, "A method of forming optical diffusers of simple known statistical properties," Opt. Acta **25,** 765–775 (1978).
35. J. W. Goodman, "Statistical properties of speckle patterns," in *Laser Speckle and Related Phenomena,* 2nd ed., J. C. Dainty, ed. (Springer-Verlag, Berlin, 1984).
36. See Sec. 5 of Ref. 2.
37. M. Nieto-Vesperinas, "Radiometry of rough surfaces," Opt. Acta **29,** 961–971 (1982).
38. Equation (35) in Sec. 5.3 of Ref. 2.
39. F. G. Bass and I. M. Fuks, *Wave Scattering from Statistically Rough Surfaces* (Pergamon, New York, 1979).
40. Equation (48) in Sec. 5.3 of Ref. 2.
41. See Chap. 7 of Ref. 39.
42. G. S. Brown, "The validity of shadowing corrections in rough surface scattering," Radio Sci. **19,** 1461–1468 (1984).
43. E. R. Mendez and K. A. O'Donnell, "Observation of depolarization and backscattering enhancement in light scattering from Gaussian random surfaces," Opt. Commun. **61,** 91–95 (1987).
44. See Chap. 2 of Ref. 39.
45. Somewhat similar patterns have also been attributed to multiple scattering by S. R. Pal and A. I. Carswell, "Polarization anisotropy in lidar multiple scattering from atmospheric clouds," Appl. Opt. **24,** 3464–3471 (1985).
46. P. Oetking, "Photometric studies of diffusely reflecting surfaces with applications to the brightness of the moon," J. Geophys. Res. **71,** 2505–2513 (1966).
47. W. G. Egan and T. Hilgeman, "Retroreflectance measurements of photometric standards and coatings," Appl. Opt. **15,** 1845–1849 (1976).
48. F. Becker, P. Ramanantsizehena, and M. Stoll, "Angular variation of the bidirectional reflectance of bare soils in the thermal infrared band," Appl. Opt. **24,** 365–375 (1985).
49. D. A. de Wolf, "Electromagnetic reflection from an extended turbulent medium: cumulative forward-scatter single-backscatter approximation," IEEE Trans. Antennas Propag. **AP-19,** 254–262 (1971).
50. Y. Kuga and A. Ishimaru, "Retroreflectance from a dense distribution of spherical particles," J. Opt. Soc. Am. A **1,** 831–835 (1984).
51. L. Tsang and A. Ishimaru, "Backscattering enhancement of random discrete scatterers," J. Opt. Soc. Am. A **1,** 836–839 (1984).
52. M. P. van Albada and A. Langendijk, "Observation of weak localization of light in a random medium," Phys. Rev. Lett. **55,** 2692–2695 (1985).
53. P. E. Wolf and G. Maret, "Weak localization and coherent backscattering of photons in disordered media," Phys. Rev. Lett. **55,** 2696–2699 (1985).
54. E. Akkermans, P. E. Wolf, and R. Maynard, "Coherent backscattering of light by disordered media: analysis of the peak line shape," Phys. Rev. Lett. **56,** 1471–1474 (1986).
55. S. Etemad, R. Thompson, and M. J. Andrejeco, "Weak localization of photons: universal fluctuations and ensemble averaging," Phys. Rev. Lett. **57,** 575–578 (1986).
56. S. Chakravarty and A. Schmid, "Weak localization: the quasiclassical theory of electrons in a random potential," Phys. Rep. **140,** 193–236 (1986).
57. A. R. McGurn, A. A. Maradudin, and V. Celli, "Localization effects in the scattering of light from a randomly rough grating," Phys. Rev. B **31,** 4866–4871 (1985).
58. D. E. Khmel'nitskii, "Localization and coherent scattering of electrons," Physica **126B,** 235–241 (1984).
59. M. Born and E. Wolf, *Principles of Optics,* 6th ed. (Pergamon, New York, 1980).